Manufacturing Surface Hardened Components of 42CrMo4 by Water-Air Spray Cooling

T. Gretzki[1)], C. Krause[1)], I. Frolov[1)], T. Hassel[1)], M. Nicolaus[1)], Fr.-W. Bach[1)], M. Kästner[2)], O. Abo-Namous[2)], E. Reithmeier[2)]

[1)] Institute of Materials Science, Leibniz University Hannover, An der Universität 2, 30823 Garbsen, Germany; gretzki@iw.uni-hannover.de
[2)] Institute of Measurement and Control Engineering, Leibniz University Hannover, Nienburger Straße 17, 30167 Hannover, Germany
[2)] National Metallurgical Academy of Ukraine, Gagarin Avenue 4, Dniepropetrovsk, 49000, Ukraine.

By employing integrated heat-treatment using forging heat, a significant shortening of the process chain is attained for manufacturing precision forged components with considerable savings in time and energy. With the aid of water-air spray cooling, surface hardening and tempering can be carried out without, at the same time, reheating the component following quenching. In this work, geometric models of splines and single cylinder crankshafts (both made of 1.7225) were surface hardened and tempered using a purpose-built rotating spray unit. The obtained hardness, microstructures and their distortions were investigated. To optically and spatially detect the components, fringe and shadow projection systems were employed. In a second research topic, the influence of the spray parameters on the component's distortion was investigated. For both components; the splined shaft and the crankshaft geometries, it was possible to carry out successful surface heat-treatments using these processes.

Keywords: precision forging, integrated heat-treatment, spray cooling, 42CrMo4

DOI: 10.2374/SRI09SP131, submitted on 11 November 2008, accepted on 2 October 2009

Introduction

The successful heat-treatment of gear wheels using water-air spaying by exploiting the forging heat leads to a shortening of the process chain, and therefore to the production costs, for manufacturing surface hardened components [1,2]. A successful industrial implementation of this technology requires that the newly acquired knowledge for quenching gear wheels be transferred to the heat-treatment of long components. A splined shaft and a single-cylinder crankshaft were chosen as example components. In order to be able to heat-treat long components using the spraying field, suitable equipment was developed and constructed. The aim was to characterise the employed spray to generate a reproducible heat-treating process. In order to evaluate the hardening and tempering process, hardness tests, metallographic investigations as well as distortion and residual stress measurements were performed on the components. The investigated components are made from hardening and tempering steel 42CrMo4. A surface hardening was carried out on the work pieces by employing spray cooling. A prerequisite was that the component's core remain ductile, corresponding to the specification requirements for gear-tooth components (in the case of the involute-splined shaft); that is the core exhibits a hardness value of less than 450 HV. In comparison to gearing systems, the splined shaft's shank is also subjected to a different loading profile. This results in a lower surface hardness requirement of approx. 500 HV. In order to meet the requirements, the investigated crankshaft has to exhibit a surface hardness of 48 HRC (below 40 HRC if it is to be subsequently rolled). Considerations for tempering from the residual heat as well as compensations for distortion by means of heat-treatment were provided for both components.

Materials and Methods

Materials, component geometry and spray field. The Investigations for the surface hardening are performed on 42CrMo4 components, which exist as model geometries in the turned condition and as forged parts. In order to carry out the test series in the spray field, a geometric model of the splined shaft (without teeth) as well as a machined single-cylinder crankshaft was used. Surface-hardening tests from the forging heat were performed by using precision forged splined shafts (**Figure** 1).

The spray field. Figure 2 depicts the configuration of the spray-cooling equipment as well as the data and material flow.

For surface-hardening of long components a new spray field was designed and constructed. The heat-treatment of long components, such as splined shafts or crankshafts, necessitates quenching at several planes, where the following requirements of such a spray field are demanded:

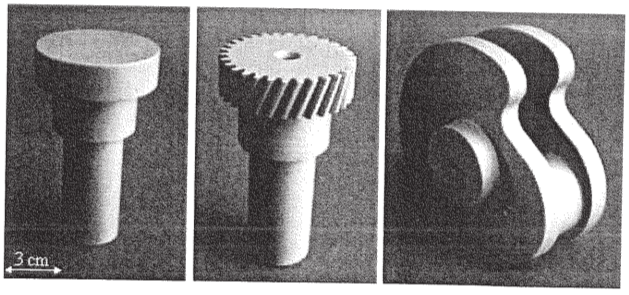

Figure 1. Splined shaft model geometry (left), single-cylinder crankshaft (right) and precision forged splined shaft (centre).

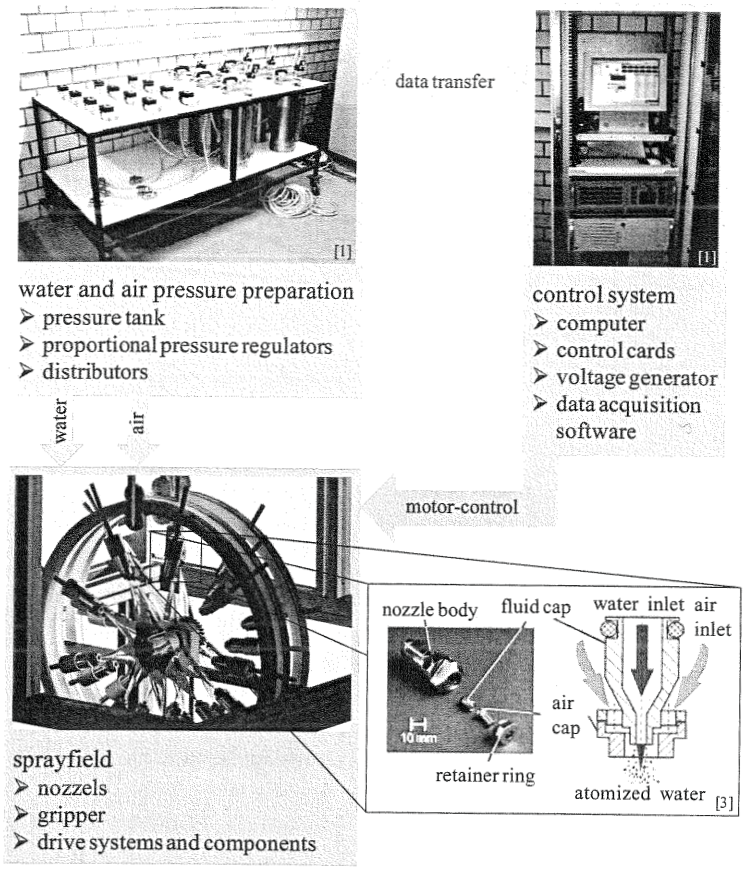

Figure 2. Schematic of spray cooling process and equipment.

- The use of two-component nozzles (water/air).
- Variable number of nozzles possessing adjustable nozzle separation distance.
- Rotation axis for the nozzle field to turn about the component.
- Adjustable for different long-components like, e.g. splined shafts and crankshafts.
- Separate drives for the individual nozzles to enable the heat-treatment of different regions of the component.

Based on these requirements, the spray field was constructed to conform to the geometries of the splined and crankshafts used here (see Figure 1) so that, by virtue of the component's rotational symmetry, a nozzle cluster having a circular nozzle configuration was chosen.

However, since the eccentricity of the crankshaft's big-end bearing excluded the rotation of the component in the spray field during the heat-treatment, the equipment is operated using an eccentric, rotating nozzle ring. The aluminium nozzle rings have an external diameter of 500 mm and each can be fitted with nine, two-component nozzles. The nozzle separation-distance is adjustable via the connection to the carrier ring. The nozzle field is rotated by a stepping motor via a belt drive. The components are held by a titanium clamping mechanism in the spray field during the heat-treatment to minimise heat conduction via the grips. Two (1 for the splines; 1 for the shank) and three (2 for the main bearings; 1 for the big-end bearing) nozzle rings are needed for heat-treating the splined and crankshafts, respectively.

The most important parameters for spray cooling are water pressure, air pressure and cooling time. These influencing parameters determine the cooling rate at the component's surface region and thereby the resulting microstructure, the size and geometric changes as well as the hardness distribution. For this reason, the following requirements are demanded of the water and compressed air supplies:

- Rapid, precise and continuous control of the water and air pressures during the test period.
- On/off switching for the pneumatic control during the equipment's operation.
- Presence of a water reservoir in the pressure vessel to continuously operate the equipment at a constant water pressure during the spraying.

The water is supplied from the pressure vessel via an ascending pipe. The rapidly responding and adaptable controller is provided via a proportional-pressure control valve, in which an electrical set-value of 0 V – 10 V corresponds to a specific pressure of 0 MPa – 0.6 MPa. In order to be able to specifically influence the residual stresses and distortion, it must be ensured that individual, or several, two-component nozzles within one carrier ring can be activated using different parameters. This is provided by controlling a total of 6 independent flow loops. For this purpose, the flow loops are controlled using a total of 12 proportional-pressure control valves and 6, 3/2-port directional valves. Manifolds for the pressure, pneumatic control and water are located at the end of the flow loops. The nozzles are directly connected to the manifolds via hose connectors. The feedback control for the water and compressed air supplies is performed via a program using the control and measuring software DasyLab 9.0.

Heat-treatment of the splined shaft and crankshaft geometries. Heat-treatment tests using the forging heat were carried out at a forging temperature of 1200 °C. The components, which were not directly heat-treated using the forging heat, were heated to 950 °C in a standby furnace since the forged components exhibited this temperature after the deformation process [4]. Following this, the splined and crankshafts were held in the spraying field and quenched. In this way, the outer surface layer is cooled to a temperature of less than 300 °C. Care was taken that the core temperature is not too high since the residual heat was used for tempering the surface layer. If the tempering temperature is too high, then the required hardness can't be obtained.

Two water-air nozzle combinations from Spraying Systems© were employed to cool the components: the circular-jet nozzle combination PAJ73160 (air nozzle) with PFJ2850 (water nozzle) and the flat fan nozzle pair J125328 (air nozzle) with J40100 (water nozzle).

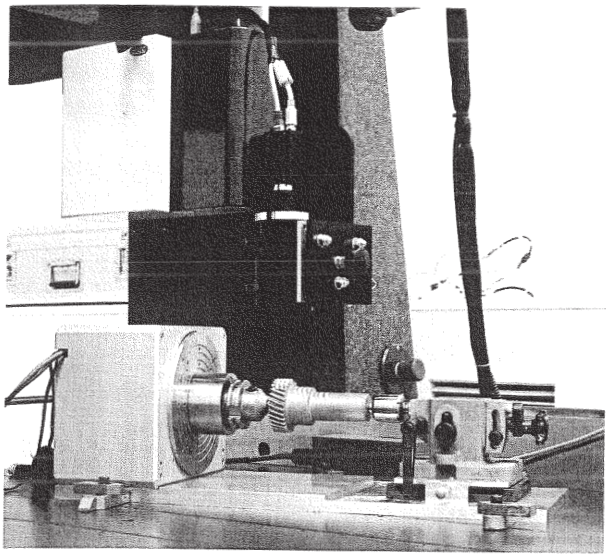

Figure 3. System set-up for detecting the spatial geometry of precision-forged pinion shafts.

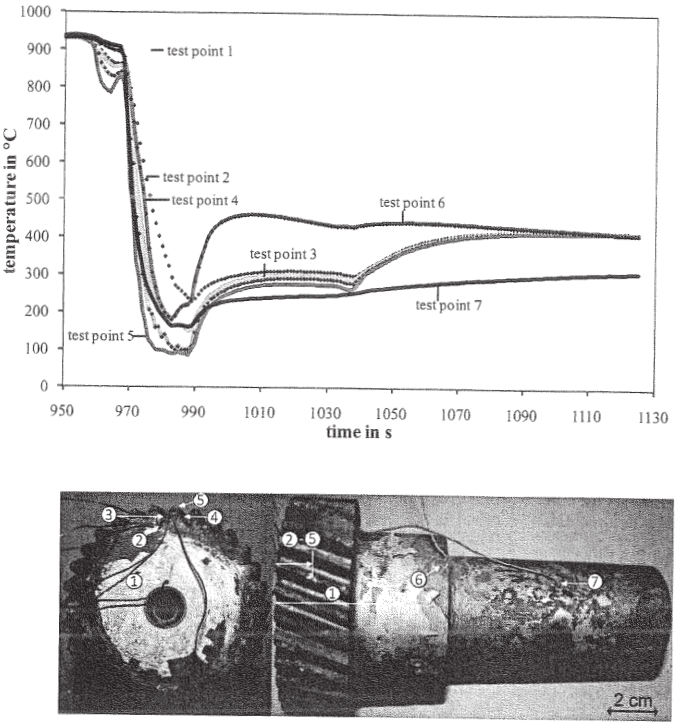

Figure 4. Temperature-time curves for surface hardening of a splined shaft.

In order to analyse the temperature profile during the heat-treatment in the spray field, thermocouple measurements were taken. For this purpose, 0.6 mm diameter holes were drilled into the components at the locations to be investigated. The 0.5 mm diameter, type K sheathed thermocouples were positioned in the drilled holes for the measurements. The data acquisition was performed by a PC via an external amplifier using an A/D converting-processor. By using the application software "DasyLab", the processing and evaluation of the measured results were able to be carried out. The investigations of the heat transfer in the actual components were accompanied by thermographic images so that the component's cooling could be monitored online.

Measurement of distortion. To characterise the quenching distortions, it is necessary to record the geometry of the component to be investigated both before and after the heat-treatment. For this purpose, an optical pinion-shaft measuring system is employed which consists of a fringe-projection sensor, a precision rotation axis with air-bearings and a gripping device. The entire measurement set-up, as depicted in **Figure 3**, is integrated into coordinate measuring equipment made by the company Werth Messtechnik GmbH. By means of this, exact and adaptable positioning of fringe-projection sensors is made possible at each measuring position.

The spatial geometric information obtained in this way must be compared in order to compute the distortion related geometric changes. To be able to carry out this comparison, the software package Polyworks is employed. With respect to this, the geometric data obtained before and after heat-treatment, which exist as scatter-plots, has to firstly be transformed into a polygonal model.

By using the Polywork's module IMInspect, the polygonal model of the post heat-treatment measured data is fitted onto the pre heat-treatment measured data, which is considered as the reference data. The deviations of the models from each other are subsequently computed orthogonal to the surface of the reference model. This gives information about the distortions caused by the heat-treatment.

A colour-coded 3D representation of the geometric changes is particularly suitable for a qualitative evaluation of the quenching distortions. By means of this, the systematic deviations typical for quenching distortions can be rapidly and reliably discerned; their characteristics can also be estimated and assessed.

Results

Temperature profile - Splined shaft. Figure 4 shows an example of a temperature-time curve for surface hardening the splined shaft at the different measuring locations. Thermocouple 1 is located in the middle of the shoulder between the spline's gear teeth and the shank. The holes for thermocouples 2 to 5 are drilled to a depth of half the width of the teeth and the holes for thermocouples 6 and 7 are drilled to a radial depth of 5 mm.

During the first phase of the cooling, in which high water and air pressures were used, the temperature in the gear teeth and at the shank's surface dropped significantly below the martensite start-temperature (approx. 370 °C). The lowest cooling rate occurred in the shoulder which was not directly exposed to the spray. The second phase of the cooling, in which it was attempted to maintain the temperature of the surface region to be hardened at an adequate level, and during which the component's interior

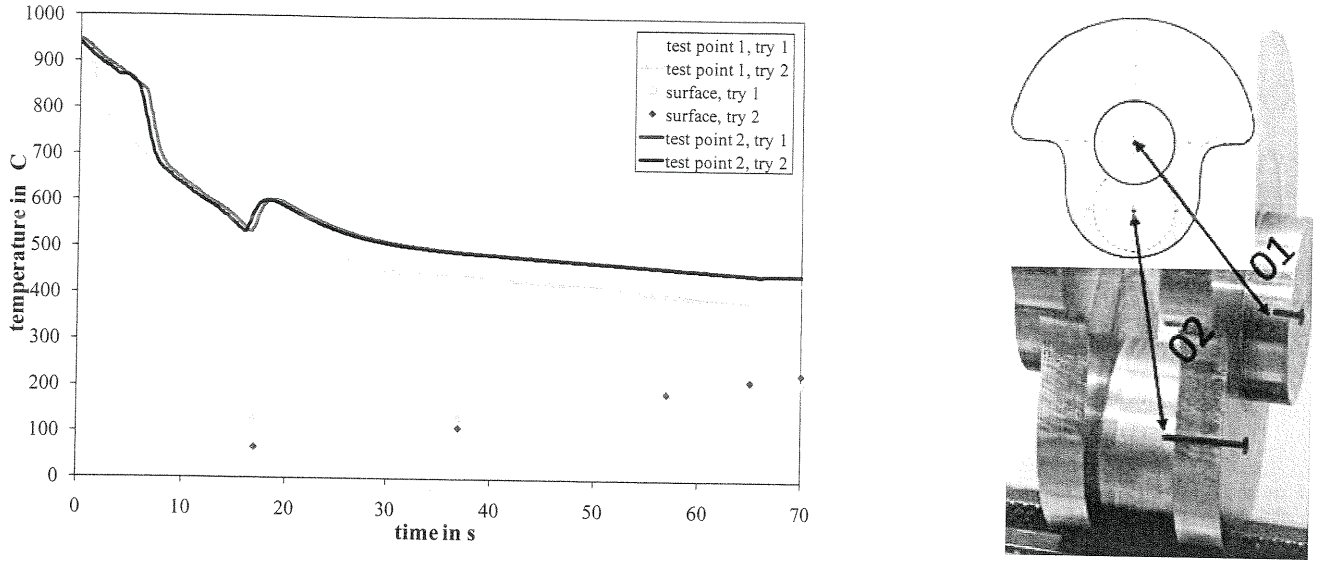

Figure 5. Temperature-time curves for surface hardening a crankshaft geometry (left); test point at the crankshaft (right).

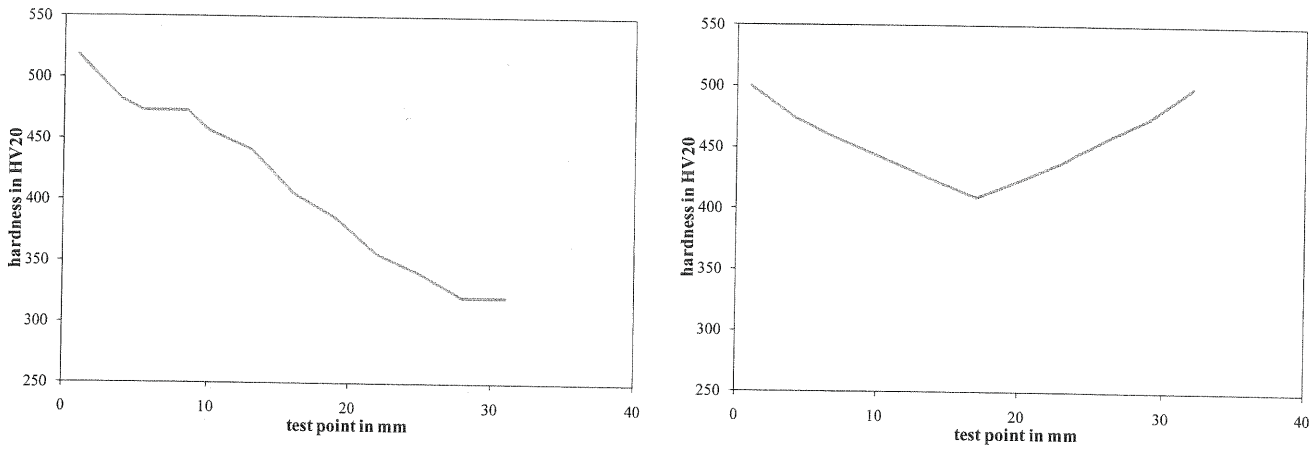

Figure 6. Hardness profile of a 42CrMo4 splined shaft hardened in the spray field in the gear teeth (left) and hardness profile for the shank's mid cross-section (right).

should slowly cool, is characterised by a temperature rise of approx. 100 °C in the teeth. A marked rise in temperature occurred in the shoulder (approx. 200 °C), whilst the lowest increase was registered at the shank's surface (50 °C). The temperatures were maintained at approximately a constant level during the second quenching phase. After this second period, the quenching process is completed and the heat gradually flows back to the component's surface region. The residual heat (temperature of approx. 425 °C) is utilised to temper the previously hardened surface layer.

Crankshaft geometry. In **Figure 5,** the temperature profile is depicted during heat-treating the single-cylinder crankshaft geometry. Specimen 1 describes the main bearing whilst specimen 2 relates to the big-end bearing. Thermocouples were positioned within the component's interior and the temperature was measured directly on the bearing surface. The surface region was rapidly cooled in order to form martensite. Contrastingly, the component's interior cooled relatively slowly. After stopping the spray cooling, the heat flows back into the surface region and tempers the martensite.

Hardness profile and microstructural changes in the Splined shaft. Before the splined shafts were cooled in the spray field, investigations had previously been carried out on the model components. Different sets of parameters were employed for the cooling of the model geometry and the splined shaft. This results in different hardness profiles in the component. The surface hardness is approx. 550 HV 30. According to DIN 50190, the hardness depth in the tooth region amounts to approx. 9 mm with a hardness limit of 475 HV. The shank's hardness does not fall below the hardness limit. The microstructural gradient, and therefore the hardness gradient, is not proportionately so clearly formed. The spray parameters, which demonstrated the best results when applied to the model geometry, were subsequently employed on cooling the splined shaft.

Figure 6 shows the hardness profiles of a splined shaft hardened in the spray field. According to DIN 50190, the hardness limit in the gear tooth region is 425 HV in the tooth and is 400 HV in central region of the shank. The resulting hardness depth in the tooth is approx. 15 mm. The hardness limit is not attained in the region of the shank, as for the pinion shaft, because of the comparatively low gradient.

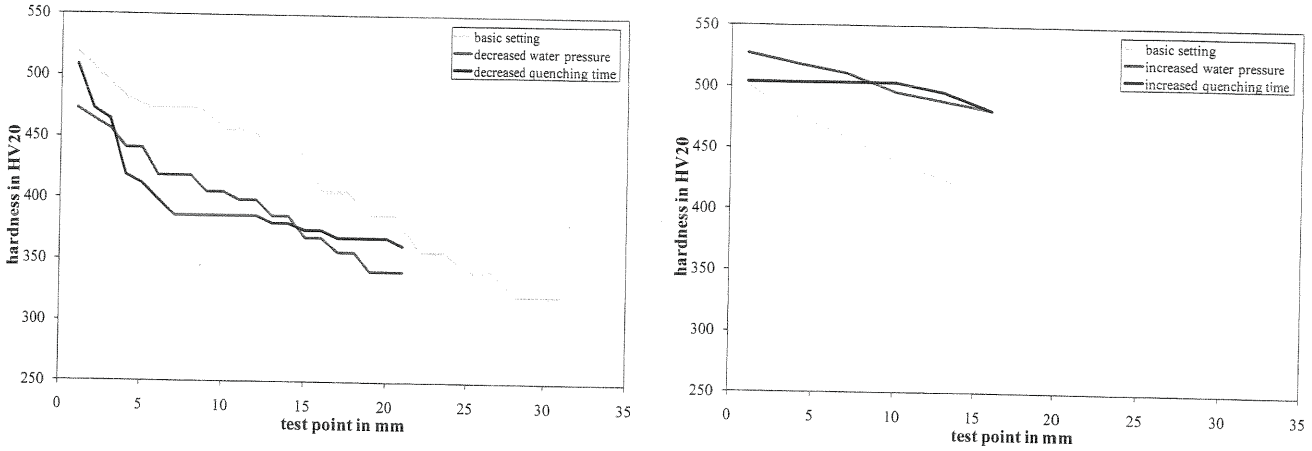

Figure 7. Hardness profiles in 42CrMo4 splined shafts hardened in the spray field with various water pressures and spraying durations. Left: Hardness profile in gear teeth, right: hardness profile in shank's mid cross section.

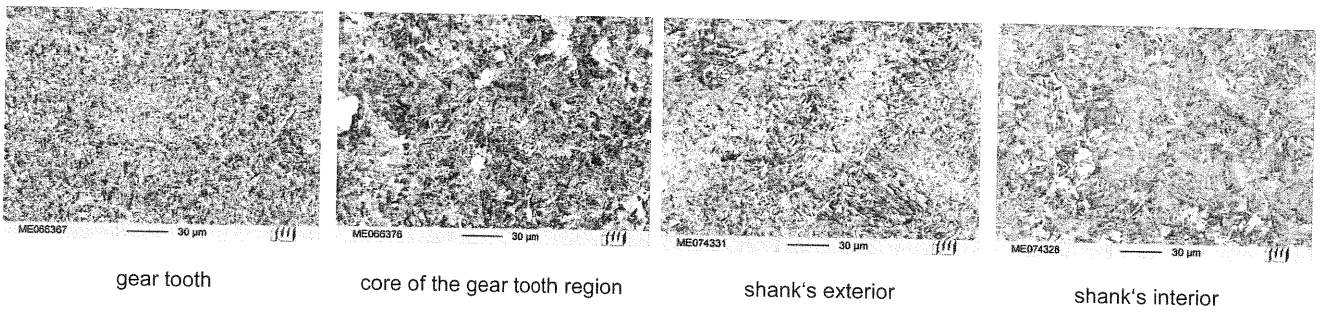

Figure 8. Microstructure of the 42CrMo4 splined shafts following heat-treatment in the spray field; etched in 2% nitric acid.

In the shank's region, the hardness profile varies in the longitudinal direction due to an inhomogeneous temperature distribution in the component. The temperature gradient results from the uncooled shoulder between the shank and the geared region. The shoulder represents a heat source which could not be continuously cooled. At this location, the splined shaft was held in the spray field. In the geared region, the effect is comparatively small and can be neglected. Near to the shoulder, lower hardness values were obtained than those at the shank's end [5]. In the surface region, the deviations from one end to the other have a maximum of 130 HV 30.

In **Figure 7**, 3 hardness profiles each in the gear teeth and in the shank's mid section are compared. The configuration of the outlet pressures were the parameters with which the splined shaft's hardness-depth profiles, depicted above, were obtained. It is clear from these graphs that a change in the water pressure raises or lowers the hardness profile. An increase in pressure causes a rise whilst a lower water pressure leads to a decrease. The pressure variations in these tests amounted to 0.1 MPa. In contrast to this, one changes the hardness depth by varying the cooling duration. A longer quenching duration leads to an increase in the hardness depth and a shorter cooling duration to a shallower depth. In the investigations performed here, the quenching duration was varied by 5 s.

Figure 8 shows the microstructure produced by the heat-treatment. In the tooth, a typical hardened microstructure is shown possessing the characteristic fine distribution of carbides. A similar microstructure is shown in the shank's surface region. In the interior of the geared region and also in the shank, a mainly bainitic microstructure is formed.

Comparison with conventional hardening procedures. In order to be able to evaluate the use of spray cooling for surface hardening geared components, a few components were industrially heat-treated using flame and induction hardening and then subsequently investigated. Since no industrial equipment was available for the investigated components, which could simultaneously heat-treat both the geared region and shank, only the geared region is considered here.

In **Figure 9**, the hardness-depth profiles are plotted for the 3 heat-treatment procedures. The surface hardness obtained from the treatment using the spray field turns out to be comparatively low though surface hardness values up to 815 HV0.05 have been achieved during hardening at previous investigations. The hardness gradient continuously falls with distance from the tooth tip. An abrupt drop in hardness at approx. 10 mm depth is found in both the industrially employed procedures. The flame hardened pinion shaft possesses the highest surface hardness. However in this case, the hardness value falls by approx. 100 HV even before the drop just mentioned. The fall occurs at approx. 7 mm. The primary hardness for both conventional procedures is approx. 300 HV. The hardness gradient of the splined shaft hardened in the spray field stabilises a little above 300 HV [1].

The flame hardened pinion shafts possess a region between the surface and the ductile core structure which, in the etched specimen, appears as a relatively wide, bright

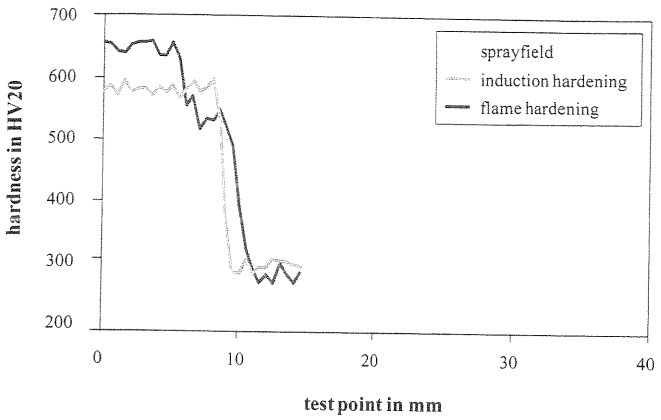

Figure 9. A comparison of the hardness-depth profile of hardened pinion shafts made from 42CrMo4.

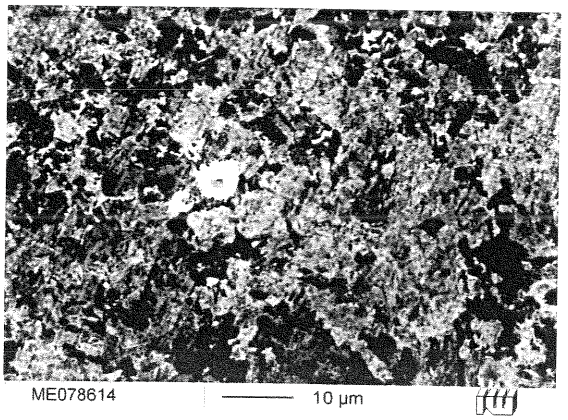

Figure 11. Transition zone "bright seam"; etchant according to Klemm.

seam (**Figure 10**). This region relates to the first abrupt hardness drop in the hardness-depth profile of the flame-hardened gearing.

In order to properly characterise the microstructure of this zone, the specimen was prepared using an etchant according to Klemm. In the micrograph in **Figure 11**, regions can be discerned which appear black. On etching with 2 % nitric acid, these areas are characterised by a white colouration. These are untextured martensite which is embedded in a bainitic microstructure. The bright spot in Figure 11indicates manganese sulphide inclusions in the material. The microstructure in the gear tooth is martensitic. The geared region's core of the investigated shaft consists of fine bainitic needles.

The induction heat-treated components (**Figure 12**) also possess a transition layer between the hardened surface and the core which is also characterised by untextured martensite located in a bainitic matrix. However, the region is not as clearly pronounced as that in flame hardening. The microstructure in the geared teeth is characterised by a hardened structure possessing fine carbide precipitates. The pinion shaft's core consists mainly of fine bainitic needles such as that following flame hardening.

Crankshaft geometry. The hardness measurements following the initial heat-treatment are depicted in **Figure 13**. This shows an inhomogeneous pattern of hardness. The hardness values within one series of measurements fluctuate and there are large differences between the measurements' series. The difference in values between the interior and exterior is up to 120 HV.

Owing to an inhomogeneous temperature distribution in the region of the main bearing, the hardness profile

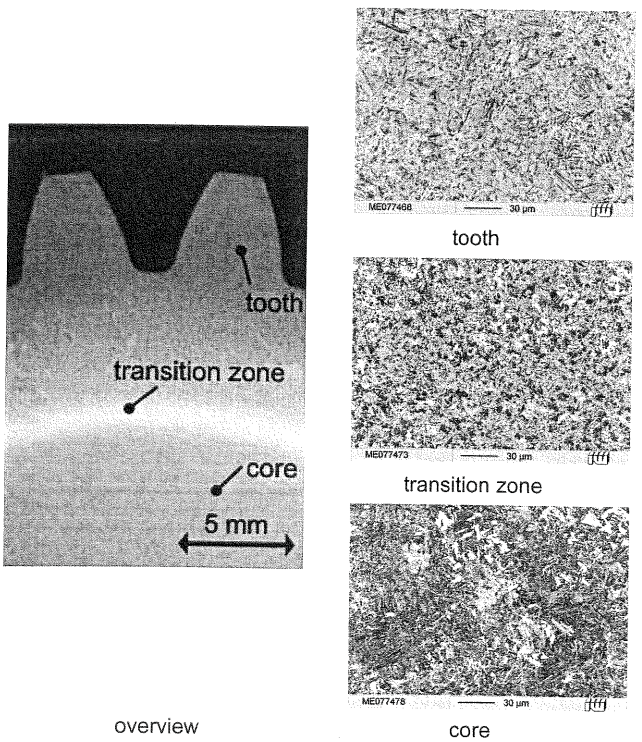

Figure 10. Microstructure of hardened 42CrMo4 pinion shafts following flame hardening; etched in 2 % nitric acid.

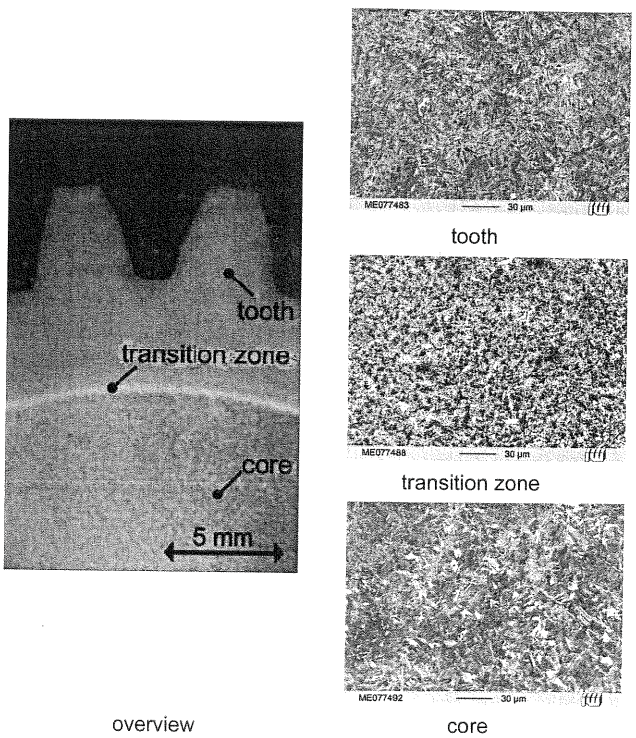

Figure 12. Microstructure of hardened 42CrMo4 pinion shafts following induction hardening; etched in 2 % nitric acid.

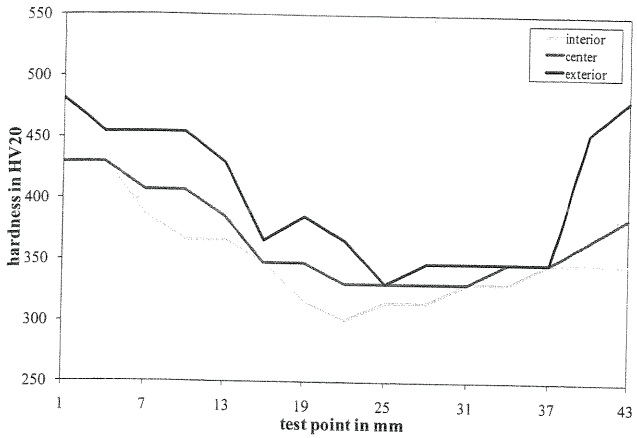

Figure 13. Hardness profile of the 42CrMo4 crankshaft after hardening in the spray field.

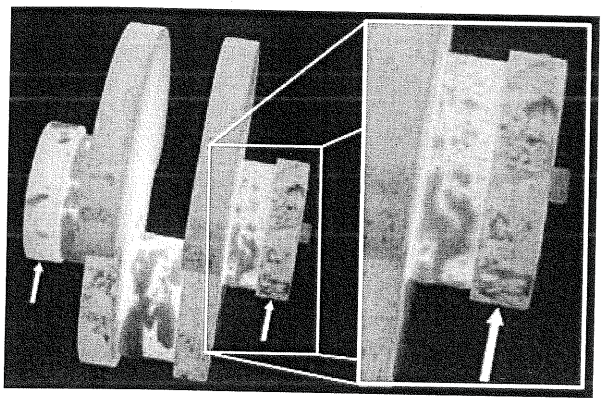

Figure 14. Austenitised crankshaft with heat shields.

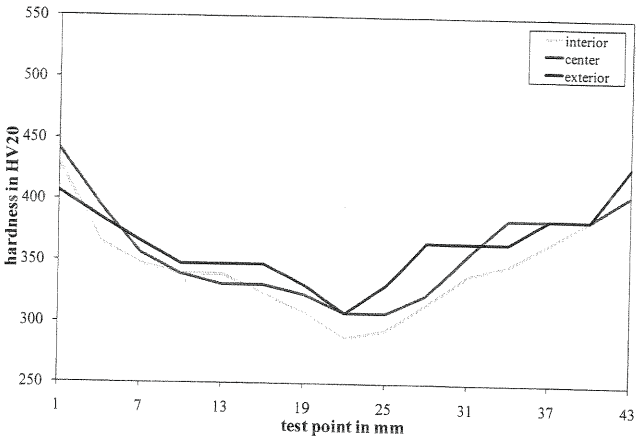

Figure 15. Hardness profiles in the bearing cross-section using the heat shields

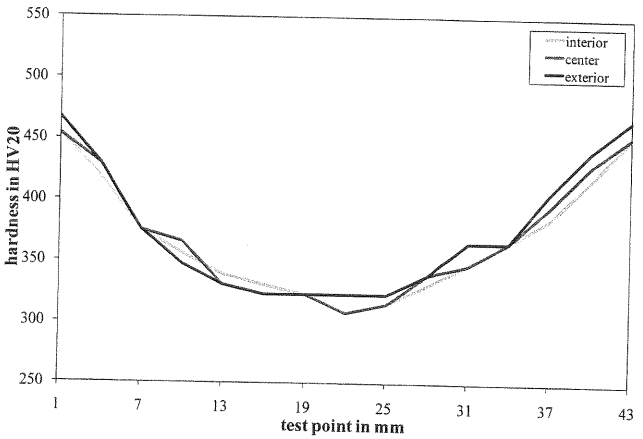

Figure 16. Hardness profile in the bearing cross-section.

varies in the transverse direction. The heterogeneity arises owing to the influence of the crank's web, which is located between the main and the big-end bearings of the crankshaft, which is not cooled. Consequently, lower hardness values are obtained near to the webs than on the outer sides. In order to compensate these temperature differences, and therefore the associated more rapid cooling, the heat shields discernible in the **Figure 14** were employed in the following tests. The heat shields have the same thickness as the crankshaft's webs and represent an additional heat reservoir.

The test was performed again with these shields. The results are depicted in **Figure 15**. A significant decrease in heterogeneity can be identified. Both the fluctuations as well as the difference between the curves have decreased. Owing to this improvement in the results, the remaining tests were carried out using these heat shields.

The following crankshaft was heat-treated using the optimised parameters. The differences between the series of measurements were able to be significantly reduced (**Figure 16**). The maximum difference is approx. 20 HV30. The hardness value for all specimens meets the required 450 HV 30 on the surfaces or 300 HV 30 in the core. The fluctuations within the hardness gradients of all measurement series have been reduced by virtue of the changed parameters.

The results of the circumferential hardness-testing of this crankshaft are depicted in **Figure 17**. The hardness measurements resulted in a homogeneous pattern of hardening. The maximum difference within one measurement around the circumference was 50 HV 30. This fluctuation lies within an acceptable range. Apart from a small subregion, the specified hardness was obtained all-around the circumference. The results of the metallographic investigations are explained in more detail using the big-end bearing of the crankshaft as an example.

Figure 18 shows the microstructure following heat-treatment. In the surface region, a typical hardened microstructure is discernible possessing characteristically, finely distributed carbides. Within the interior of the bearing, a mainly bainitic microstructure has formed. Further examinations show that both the transition from the main bearing to the web as well as that from the big-end bearing to the web are influenced by using spray cooling. The data points start 1 mm below the surface and have a separation of 3 mm.

The results of the hardness testing are depicted in **Figures 19 and 20**. In the transition from the main bearing to the web, a significant influence due to the spray can be identified. In this region, the hardness values rise (measurement position 10 mm and 55 mm) and then fall back. One can also observe the same influence in the transition from the big-end bearing to the web (see measure-

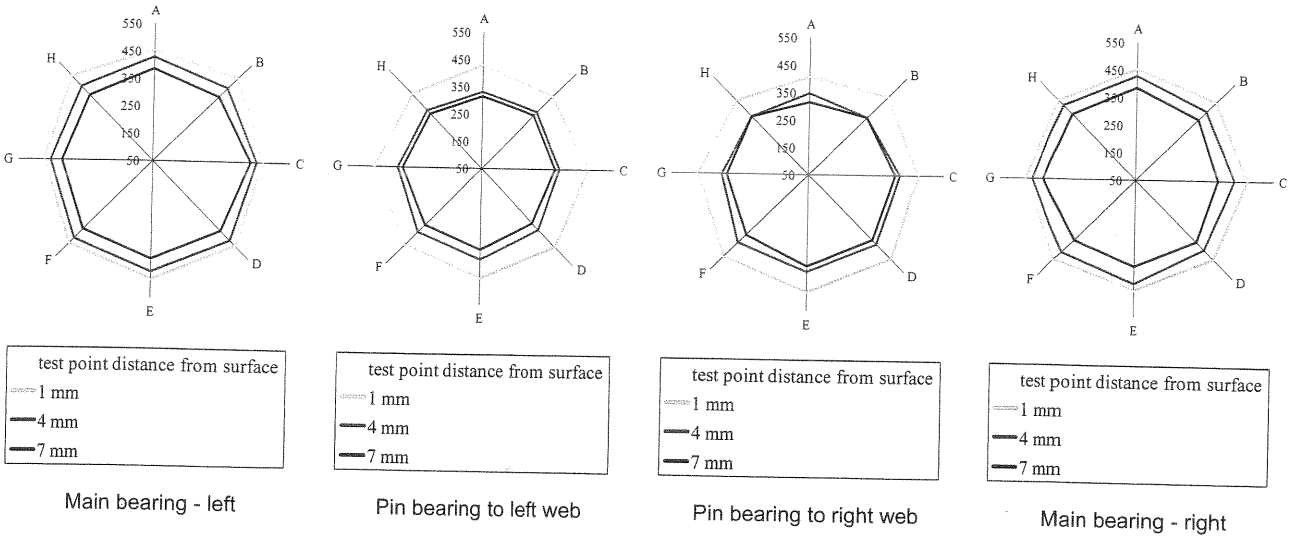

Figure 17. Circumferential hardness testing.

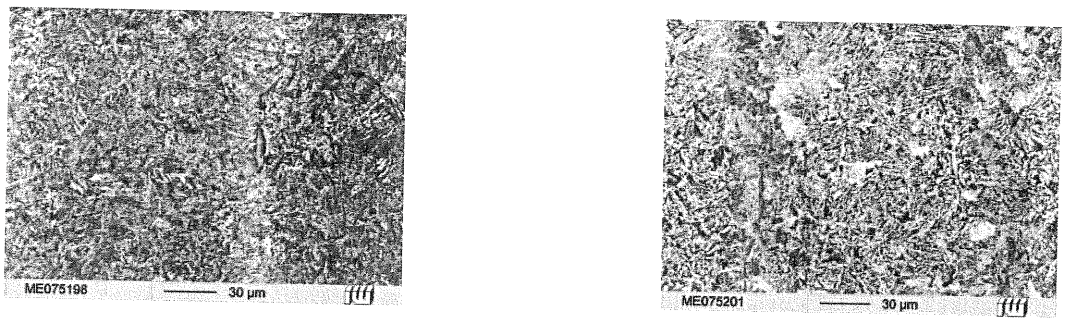

Figure 18. Microstructure following heat treatment. Left: surface region and right: specimen's centre.

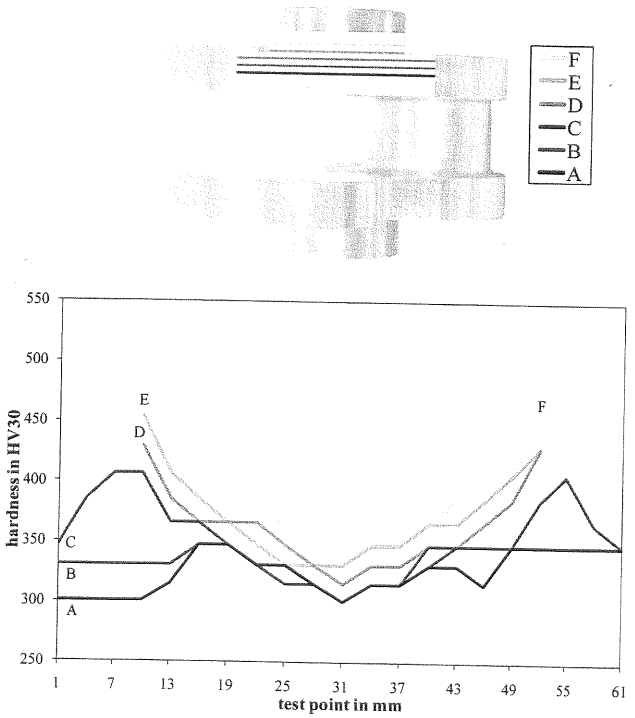

Figure 19. Top: Schematic representation of the measurement series or measurement positions, main bearing-web. Bottom: Hardness profile at the transition from the main bearing to the web.

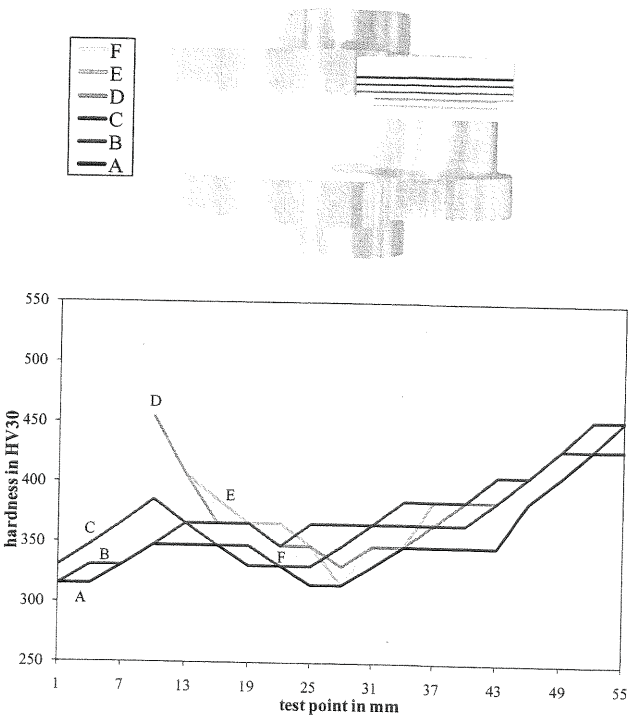

Figure 20. Top: Schematic representation of the measurement series or measurement positions, big-end bearing-web. Bottom: Hardness profile at the transition from the big-end bearing to the web.

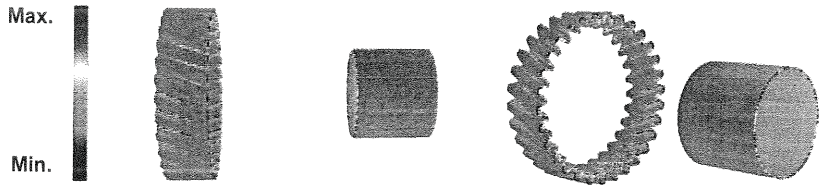

Figure 21. Colour-coded representation of quenching distortion for a pinion shaft heat-treated using a two-phase spray.

ment position 10 mm in the diagram). Even from the measurement position 46 mm onwards, the same hardness values are obtained as those in the surface region of the big-end bearing. This is because the web in this region has approx. the same geometry as the big-end bearing. In the web's region of unbalance, the hardness value again sinks to the primary value. According to [6], the crankshaft's fatigue strength is increased by this influence of the web.

Distortion. Figure 21 shows, in the form of a three-dimensional colour-coded geometric model, the distortion related geometric changes of a pinion shaft hardened in the spray field.

The pinion shaft's gear teeth exhibit a homogeneous and small distortion. A small deviation in the helical angle is noticeable. In the partial image (b), the helical angle of the hardened gear teeth is larger on the left side of the pinion shaft's gear teeth, and on the right side of the figure, the hardened gear teeth exhibit a smaller helical angle than that of the unhardened reference. The maximum geometric changes in the gear teeth are in the range of approx. 75 µm. Moreover, it can be established that the bearing seat's radius of the pinion shaft is approx. 30 µm smaller subsequent to hardening than that before hardening.

The quenching distortions of the bearing seat can be characterised by both determining the cylindricity as well as evaluating the cylinder's radius. Evaluating the coaxiality of the bearing seat with the pinion shaft's gear teeth axis is particularly suitable for examining the distortions of the entire component. During the examination of the pinion shaft depicted in Figure 20 the parameters given in **Table 1** were determined before and after the hardening. It is noticeable that the deviation of coaxiality of the bearing seat and the gear teeth axis significantly increase due to the hardening process, whilst the deviation of the bearing seat from its cylindrical form becomes smaller. Furthermore, it must be mentioned that the radius of the bearing seat assumes a smaller value after hardening than that before hardening. This effect can presumably be attributed to changes of the residual stress relations in the component due to the heat-treatment.

The quenching distortions of the pinion shaft's gear teeth can, for example, be characterised by determining the parameters for spatially assessing the gear teeth deviations, which was developed within the collaborative research centre 489.

In this context the project aims to devise a testing method for measuring finished components by means of an optical instrument. Owing to their reflectiveness, the surfaces of finished components are unsuited to measurements using optical techniques. This is to be remedied by a selection of surface treatment methods. A demonstration device was constructed as a product of the transfer project, which treated component's surfaces under manufacturing conditions and completely measured the component using fringe-projection sensors.

Investigations of optical cooperativity were carried out on different component surfaces. In addition to this, both features of optically cooperative surfaces as well as methods for measuring optical cooperativity were identified though theoretical considerations and reflective models of engineering materials.

In order to produce optically cooperative surfaces, the methods of surface and thin-coating technology are implemented. Among these number physical methods such as PVD technology, (electro-)chemical treatment as, for example, electrochemical etching and electroless coatings as well as mechanical treatments of the components by means of glass-bead and corundum blasting (**Table 2**). The processes mentioned are suitable for producing optically cooperative surfaces since, owing to the corresponding test parameters, a change of the component's surface occurs at the sub-micrometer scale. Currently, no indication in the literature is provided that such processes are employed for manufacturing optically cooperative surfaces.

The behaviour of the blast specimens was determined by means of a simple goniometric reflecting attachment [7]. In this way it is shown that blasting using the fused alumina gives good results. Also, electrochemical etching

Table 1. Parameters for quantifying the geometric deviations of the pinion shaft's bearing seat before and after hardening.

Parameters	Unhardened	Hardened
Radius of bearing seat, mm	17.787	17.746
Cylindricity, mm	0.024	0.017
Coaxiality, mm	0.089	0.123

Table 2. Surface treatment methods for manufacturing optically cooperative surfaces on polished cylindrical specimens of the case hardening steel 16MnCrS5.

Treatment methods	Parameter
Blasting with fused alumina EKF1000	0.3 MPa- 0.6 MPa blasting pressure
PVD etched with argon/nitrogen plasma	2.5 h, HF power 700 W – 1400 W
Etched in 20 % H_2SO_4	1 min – 15 min
Electrochemically etched in NaCl solution (5 %)	1 min – 15 min, 1A anodic/cathodic
Electrochemically etched in 1 M HCl	1 min – 15 min, 2A anodic
Chemically copper-plated	1 h, various additives

using 1-M HCl demonstrates, to some extent, promising results. For the purpose of optical cooperativity, the specimens treated in this way exhibit an improvement which can be supported using contact and optically determined roughness values.

Discussion

The surface region of heat treated long components was initially quenched and subsequently tempered using the residual forging heat. Via the tempering duration and the temperature, the hardness of the gear teeth can be adjusted, whereby the duration plays a secondary role. Since during the heat-treatment of the splined shaft, the shoulder between the shank and the gear teeth was not hardened, heat continuously flowed from this location into the cooled regions. This effect was demonstrated particularly clearly in the region of the shank. At this location, relatively high fluctuations occur in the hardness values along its length. In the gear teeth region, this influence can be neglected. For example, this effect can be resolved by employing an additional nozzle ring in this region. As previously mention above, a higher hardness value can be achieved by lowering the tempering time during tempering from the residual heat; however, this increases the risk of crack formation since stresses are released during tempering. Cracking in the teeth of the splined shaft occasionally came about due to heat-treatment in the spray field (**Figure 22**).

In order to carry out surface hardening by using the water-air spray, high temperature gradients are required which can trigger this type of damage. The cracks can be initiated from manganese sulphide or surface defects. To avoid these undesirable effects, surface hardenable steels like, e.g. Cf53 are to be employed or a slower and graduated cooling strategy for heat-treatment are to be used in the next proposals application.

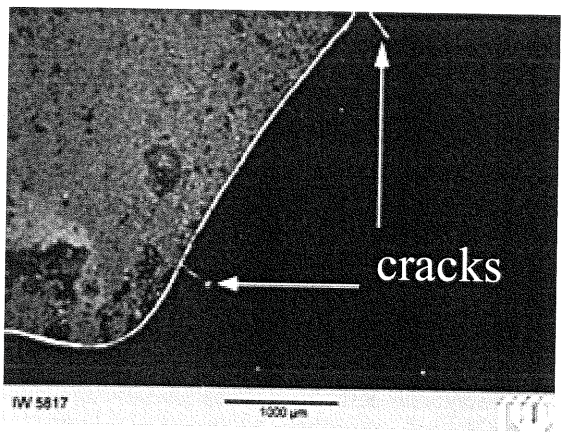

Figure 22. Cracks in a gear tooth following heat-treatment in the spray field.

Tensile residual stresses had been measured at the surface of the investigated long components. These stress conditions also contribute to the formation of cracks. A slower cooling strategy, as previously mentioned, could provide lower thermally induced residual stresses and thereby reduce this influence.

During the tests using the spray cooling, a reproducible relationship between the spray parameters and the operating hardness-depth profile was able to be observed. An increase in the water pressure during the initial cooling phase causes an increase in the surface hardness. Increasing the spraying duration during the initial phase causes an increase in the hardness depth. This relationship is valid for both the splined shaft as well as for the crankshaft.

Conclusions

Spray cooling by using a mixture of water and air is suitable for carrying out surface hardening on die-forged components. During the heat-treating process of the pinion shaft's shank, inhomogeneities in the hardness distribution occur which can be compensated by additional nozzles or by employing a heat shield.

Acknowledgements

The authors would like to thank the German Research Foundation for their financial support of the research work carried out within the scope of the Collaborative Research Centre 489.

References

[1] Krause, C.: Randschichtvergüten verzahnter Bauteile mittels einer Wasser-Luft-Spraykühlung, Dissertation Thesis, Leibniz Universität Hannover, 2008, ISBN 978-3-939026-92-1

[2] Krause, C.; Wulf , E.; Nürnberger F.; Bach, Fr.-W.: Wärmeübergangs- und Tropfencharakteristik für eine Spraykühlung im Temperaturbereich von 900 °C – 100 °C. Forschung im Ingenieurwesen, 72 (2008), No. 3, 163-173

[3] Bach, Fr.-W.; B.-A. Behrens; H. Dähndel; Chr. Krause; A. Huskic: Integration of heat treatment in precision forging of gear wheels. The Arabian Journal of Science and Engineering, 6 (2005), 103-112

[4] Bach, Fr.-W., Krause, C., Schaper, M., Nürnberger, F.: Heat treatment of precision forged steel gears by usage of the forging heat, Scientific Bulletin of the National Metallurgical Academy of Ukraine, 8 (2005), 488-493

[5] Krause, C.; Hassel, T.; Frolov, I.; Gretzki, T.; Kästner, M.; Seewig, J.; Bormann, D.; Bach, Fr.-W.: Randschichtvergüten von Zahnwellen mittels Wasser-Luft-Sprühkühlung. HTM, 63 (2008), No. 1, 22-26

[6] Berns, H., Theisen, W.: Eisenwerkstoffe: Stahl und Gusseisen, 3rd ed., Springer Verlag, 2006, p. 206 and p. 209.

[7] Abo-Namous, O., Seewig, J., Kästner, M., Reithmeier, E.: Fast Method to measure optical cooperativity. Proc. DGaO 2008, p. A16